



Cite this: *RSC Sustainability*, 2023, **1**, 1814

Hydrogenation of biodiesel catalysed by pyrazolyl nickel(II) and palladium(II) complexes†

Oluwasegun Emmanuel Olaoye, *a Olayinka Oyetunji, *a
Banothile C. E. Makhubela, b Gopendra Kumar a and James Darkwa *bc

Biodiesel from renewable sources offers an attractive alternative to conventional diesel fuel and partial hydrogenation of free-fatty acid methyl esters (FAME) is one way to improve this renewable fuel. We have used the mononuclear pyrazolyl nickel(II) and palladium(II) complexes, $[\text{NiBr}_2(\text{L}1)]$ (1), $[\text{NiBr}_2(\text{L}2)]$ (2), $[\text{NiBr}_2(\text{L}3)]$ (3), $[\text{PdCl}_2(\text{L}1)]$ (4), $[\text{PdCl}_2(\text{L}2)]$ (5) and $[\text{PdCl}_2(\text{L}3)]$ (6) (where $\text{L}1 = 3,5\text{-dimethyl-1H-pyrazole}$, $\text{L}2 = 3,5\text{-di-tert-butyl-1H-pyrazole}$ and $\text{L}3 = 5\text{-ferrocenyl-1H-pyrazole}$), as hydrogenation catalysts to improve the fuel properties of selected plant biodiesel. These nickel and palladium complexes exhibit significant catalytic activities in the selective and partial hydrogenation of biodiesel produced from *Jatropha curcas*, chinaberry (*Melia azedarach*), and *tsamma* melon (*Citrullus ecirrhosus*) seed oils. Depending on the catalyst and reaction time, a blend of un-hydrogenated, partially hydrogenated, and fully hydrogenated biodiesel was produced whose fuel properties meet the requirements of EN 14214 and ASTM D 6751 standards as fuels.

Received 26th July 2023
Accepted 1st September 2023
DOI: 10.1039/d3su00254c
rsc.li/rscsus

Sustainability spotlight

With the rapid growth in fossil fuel consumption and global warming emissions, there is an urgent need to explore green and renewable energy resources. Biodiesel presents a compelling alternative to conventional petroleum/diesel fuel; because of its well-known advantages, such as non-toxicity, the derivation from renewable feedstocks, and biodegradability. However, the properties of biodiesel are negatively affected by a high degree of unsaturation as well as full saturation, hence the need for selective and/or partial hydrogenation to improve the properties. We report the catalytic activities of pyrazolyl Ni(II) and Pd(II) complexes for the selective/partial hydrogenation of biodiesel produced from nonedible seed oils. This work addresses the following UN SDGs: Responsible Consumption and Production (SDG 12) and Climate Action (SDG 13).

1 Introduction

Hydrogenation of various chemical conversions of feedstocks to targeted products has been studied by many research groups using various transition metal compounds as either homogeneous or heterogeneous catalysts.^{1–5} Amongst the most used metals in the homogeneous catalytic hydrogenations of unsaturated compounds are ruthenium,^{6,7} osmium,⁸ cobalt,⁹ rhodium,^{10,11} iridium,² and platinum;¹² but nickel^{3–15} and palladium¹⁶ complexes stand out as metals of choice when it comes to hydrogenation of C=C bonds. Examples of nickel-catalysed homogeneous hydrogenation of C=C bonds are provided by work done by Angulo *et al.*¹⁷ Angulo and

Bouwman,¹⁸ Angulo *et al.*¹⁹ and Shevlin *et al.*²⁰ in the asymmetric hydrogenation of α,β -unsaturated esters with high enantio-selective products.

Nickel catalysts offer good catalytic activities and selectivities at a lower cost as hydrogenation catalysts. Palladium catalysts, on the other hand, though more expensive, have superior catalytic activities and selectivity in the hydrogenation of unsaturated compounds; and also provide a NMR spectroscopic handle that allows *in situ* monitoring of the hydrogenation reaction.^{21,22} Examples of palladium-catalysed reactions are provided by Pelagatti *et al.*²³ and Bacci *et al.*²⁴ for hydrazonic-phosphine (P^NO) palladium(II) complexes and Ding *et al.*²⁵ have reported P^NP palladium complexes in the transfer hydrogenation of α,β -unsaturated ketones where reactions were occurring under mild conditions and were chemo-selective.

However, because of the air and moisture sensitivity of phosphines, metal complexes with nitrogen-donor ligands are emerging as alternatives to phosphorus-donor palladium complexes as hydrogenation catalysts.²⁶ For example, {bis(arylimino)acenaphthene}palladium(0) complexes have been found to chemo-selectively hydrogenate C=C bonds in α,β -unsaturated aldehydes.²⁷ But despite numerous applications of

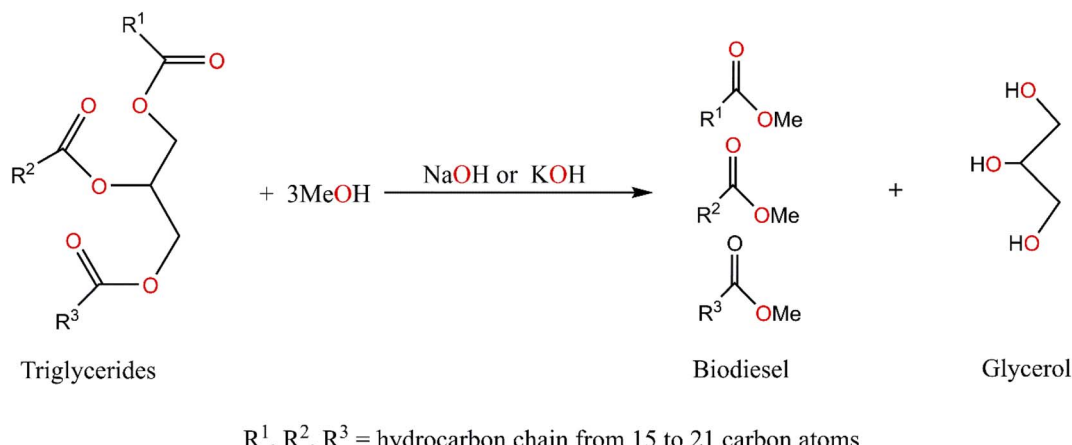
^aDepartment of Chemistry, University of Botswana, Private Bag UB 00704, Gaborone, Botswana. E-mail: 201605304@ub.ac.bw; oyetunji@gmail.com; jdarkwa@gmail.com

^bDepartment of Chemical Sciences, University of Johannesburg, Kingsway Campus, Auckland Park, 2006, South Africa

[†]Botswana Institute for Technology Research and Innovation, Machel Drive, Gaborone, Botswana

† Electronic supplementary information (ESI) available. See DOI: <https://doi.org/10.1039/d3su00254c>





Scheme 1 Transesterification of triglycerides with low molecular weight alcohol to produce free-fatty methyl esters (biodiesel).³¹

nitrogen-donor nickel(II) and palladium(II) in catalysis, little work has been reported on pyrazolyl metal complexes as catalysts for the hydrogenation of unsaturated esters, especially the long-chain free-fatty acid methyl esters (FAME).

With the depletion of fossil fuel consumption, there is an urgent need to explore green and renewable energy sources as a substitute for fossil fuels in devices where batteries are either cumbersome or impractical.²⁸ One way to solve these problems is to increase the use of bio-based fuels.²⁹ Biodiesel (Scheme 1) offers attractive alternatives to conventional petroleum diesel fuel; because of its well-known advantages, such as non-toxicity, derivation from renewable feedstocks, and biodegradability.^{30–32}

We report the partial and/or selective hydrogenation of biodiesels produced from *Jatropha curcas*, chinaberry (*Media azedarach*) and *tsamma* melon (*Citrullus ecirrhosus*) seed oils that leads to mixtures of the original un-hydrogenated biodiesel, partially hydrogenated biodiesel, and fully hydrogenated biodiesel as biodiesel blends.

2 Experimental

2.1 General information

All air and moisture-sensitive compounds were manipulated using standard Schlenk and vacuum line techniques under an argon atmosphere. Argon HP/zero-grade, and hydrogen gas HP/zero-grade (>99%) were purchased from Afrox (South Africa). Reagent grade ethyl formate (97%), acetic anhydride (99%), ferrocene (98%), hydrazine monohydrate (98%), hydrazine dihydrochloride (98%), (ethyleneglycoldimethylether)nickel(II) bromide (98%), 1,4-dioxane (99%), formic acid (95%), linoleic acid (99%) and 3,5-dimethyl-1*H*-pyrazole (**L1**) (99%) were procured from Sigma-Aldrich; while potassium hydroxide (85%) and sodium hydrogen carbonate were purchased from Promark (South Africa) and Rochelle chemicals (South Africa) respectively. Compounds 3,5-di-*tert*-butyl-1*H*-pyrazole (**L2**)³³ and 5-ferrocenyl-1*H*-pyrazole (**L3**)³⁴ and $[\text{PdCl}_2(\text{NCMe})_2]$,^{35,36} and nickel(II) and palladium(II) complexes (**1–6**)^{37,38} were synthesized according to the literature procedures.

NMR spectra were recorded on a Bruker-400 ultra-shield MHz NMR spectrometer (^1H at 400 MHz). Spectrometer

chemical shifts were reported relative to the internal standard tetramethylsilane (δ 0.00 ppm) and referenced to the residual proton and carbon signals at 7.24 ppm and 77.0 ppm respectively of CDCl_3 .

All hydrogenation reactions were performed in PPV-CTR01-CE high-pressure autoclave reactor coupled with a stirring pact, heating and cooling system.³ The hydrogenation reactions were followed by ^1H NMR spectroscopy and gas chromatography, using dioxane and methyl heptadecanoate as internal standards for hydrogenations of methyl linoleate (ML) and biodiesels respectively, which were used to determine the percentage conversions.

2.2 Synthesis of methyl linoleate (ML)

Linoleic acid (5 g, 17.83 mmol) was dissolved in methanol (20 mL) and allowed to stir for 30 min. About 7 drops of concentrated H_2SO_4 were added, and the reaction was allowed to reflux at 60–65 °C for 6 h. After the completion of the reaction, Na_2CO_3 (pH ~12) was added dropwise forming two layers of the solution. The organic layer was separated from the aqueous layer, concentrated, and dried over MgSO_4 to afford a pale-yellow oily compound. Yield: 4.7 g (90%).

2.3 Typical transesterification reaction of jatropha, chinaberry and melon seed oils

Biodiesels from three plants were produced by an alkali-catalysed transesterification reaction between the appropriate plant oil and methanol. A typical *Jatropha curcas* seed oil (JASO) transesterification reaction was performed with 45 g (52 mmol) of JASO in a 250 mL three-necked round bottom flask and heated to 60 °C. Methanol (15 g, 468 mmol) and KOH (0.45 g; 1 wt% concerning JASO) were mixed vigorously in a different flask, to obtain a homogeneous mixture before the mixture was added to the heated JASO (with approximately 6 : 1 methanol : JASO molar ratio) and stirred for 2 h. The resulting solution was then transferred into a separating funnel and left overnight to afford two layers or phases (*i.e.*, the methyl esters of JASO and glycerol). The methyl esters of JASO (biodiesel) were then washed twice with distilled water to ensure the removal of all



traces of glycerol, and unreacted methanol was removed *in vacuo* before the final product was dried over anhydrous Na_2SO_4 .

A similar procedure was used to prepare biodiesels from chinaberry (CHSO) and melon (MESO) seed oils. The compositions of free-fatty methyl esters of *Jatropha curcas*, chinaberry (*Melia azedarach*) and *tsamma* melon (*Citrullus ecirrhosus*) seed oils were determined by gas chromatography-mass spectrometry (using a Thermo Scientific TSQ series fitted GC-FID that is coupled to Triple Quadrupole Mass Spectrometer) and a TG-5MS (30 m \times 0.25 mm \times 0.25 μm) fused-silica capillary column with helium as the carrier gas at a flow rate of 1 mL min^{-1} . About 1 μL of the sample was injected into the oven (150 $^{\circ}\text{C}$) with an injector and detector of 250 $^{\circ}\text{C}$, with a split ratio of 12 : 1. The oven temperature was kept at the initial 80 $^{\circ}\text{C}$ for 2 min, and then gradually increased from 80 $^{\circ}\text{C}$ to 300 $^{\circ}\text{C}$ at the rate of 8 $^{\circ}\text{C min}^{-1}$, the total run time was 32 min. The type and the amount of each free-fatty acid methyl esters (FAME) composition were identified by reference to the retention time and calculation from the fraction of area under the peak of the FAME, respectively (Fig. S23†).

The conventional diesel fuel used for comparison in this study was purchased from a local Shell petrol depot/station and has properties including a boiling point of 149 $^{\circ}\text{C}$, a density of 845 kg m^{-3} , the viscosity of 2.7 $\text{mm}^2 \text{s}^{-1}$ at 40 $^{\circ}\text{C}$, the acid value of 0.28 mg KOH g^{-1} and calorific value of 45.6 MJ kg^{-1} .

2.4 General procedure for hydrogenation reactions

2.4.1 Hydrogenation of methyl linoleate with molecular hydrogen. Hydrogenation experiments were carried out in stainless steel reactors with magnetic stirrers. In a typical experiment, methyl linoleate (0.3 mmol), catalyst (2.5 μmol , 0.83 mol%), hydrogen gas (5 bar) and methanol (5 mL) were introduced into the stainless-steel reactor. The catalyst to methyl linoleate ratio in all cases was 1 : 120. The solution mixture was purged twice with nitrogen gas, followed by the introduction of hydrogen gas (5 bar) and the mixture was stirred at 50 $^{\circ}\text{C}$ for 3 h. After the reaction period had elapsed, the reacting vessel was cooled, and excess pressure generated was vented off slowly. Aliquots of the products were drawn from the reaction mixture at different reaction times, filtered using MS® nylon syringe filter (0.22 μm , 13 mm), and the hydrogenation products' conversions were determined by ^1H NMR spectroscopy. Due to the small scale of reactions performed, accurate isolated yields were not determined for all reactions explored. The ^1H NMR spectrum of methyl linoleate is shown in Fig. S1 and S2.† The conversions and product distributions, using dioxane as an internal standard, were determined using the integration of dioxane from NMR spectra of the reaction mixture (Fig. S22†). The nature of the products was confirmed by GC-MS.

2.4.2 Hydrogenation of biodiesel with molecular hydrogen. In a typical experiment, biodiesel (0.5 g), catalyst (5 mg, 1 wt%), hydrogen gas (10 bar) and methanol (10 mL) were introduced into a stainless-steel reactor. The solution mixture was purged twice with nitrogen gas, followed by the introduction of

hydrogen gas (10 bar) and the mixture was stirred at 50 $^{\circ}\text{C}$ for 3 h. Aliquots of the products were drawn from the reaction mixture at different reaction times, filtered using MS® nylon syringe filter (0.22 μm , 13 mm), and conversions of the hydrogenation products were determined by GC-MS, using methyl heptadecanoate as an internal standard. The % conversions of the product distributions were determined from the peak areas of each of the fatty-acid methyl esters formed.

2.5 Fuel properties analyses

The fuel properties of biodiesels produced from the three seed oils and the partially hydrogenated biodiesels were analysed for relative density, cold properties (cloud and pour points), flash point, acid value and heat of combustion (calorific value). The cloud and pour points were determined using the ASTM standard test methods (ASTM D97 and D2500). The ASTM D93 standard test method for flash point by Pensky-Martens closed cup tester was used to determine flash points of the biodiesels. The heat of combustion of the biodiesels was determined using the CAL 3K-AP Calorimeter system with an automatic data acquisition through the CalWin Calorimeter software, which determines the calorific values of samples. The acidity values of the biodiesel were measured according to the EN14104 standard test method.³⁸

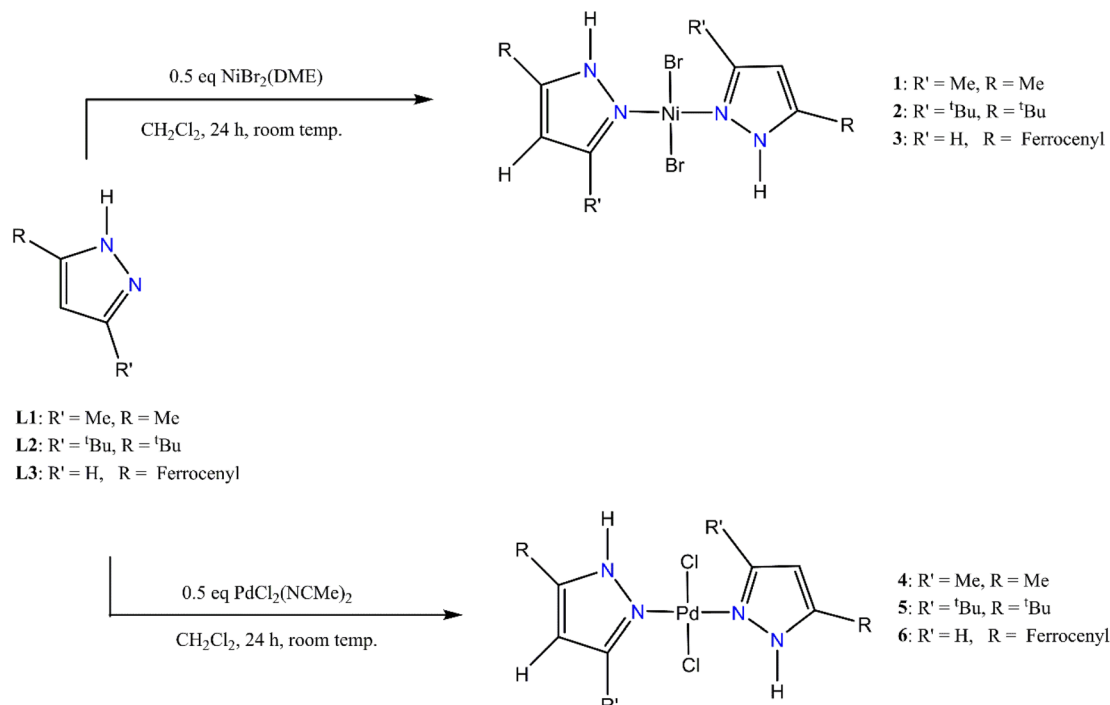
3 Results and discussion

All the pyrazolyl nickel(II) and palladium(II) complexes that were used as catalysts in this study, as illustrated in Scheme 2, are known compounds. For example, complexes 1,³⁷ 2,³⁷ 4 (ref. 39–41) and 5 (ref. 39 and 40) have been used as ethylene^{37,39} or phenylacetylene⁴⁰ polymerization catalysts and as anticancer agents⁴¹ respectively.^{42b–e} There are also several examples of bis(pyrazolyl)- nickel(II) and palladium(II) complexes in which the N-H in complexes 1–4 has been derivatised, as in complexes 3 (ref. 42a) and 6,^{42a} and used as catalysts. Some examples of bis(pyrazolyl)palladium complexes have been used as Heck and Suzuki coupling catalysts. The complexes in Scheme 2 that were used for this were fully characterised by NMR spectroscopy and in selected cases by single-crystal X-ray crystallography. Fig. S36–S43† display the ^1H and $^{13}\text{C}\{^1\text{H}\}$ NMR spectra.⁴² Fig. S44 and S45† show the X-ray crystallographic parameters for 5 and 6.⁴²

3.1 Hydrogenation reactions

3.1.1 Hydrogenation of methyl linoleate (ML). The preparation of methyl linoleate (ML) from linoleic acid was followed according to the literature procedures (Fig. S1 and S2†).⁴³ Hydrogenation of ML was used as a model reaction, first to determine which of the six nickel and palladium complexes (1–6) would have the best catalytic activity and to establish the best reaction parameters to use in hydrogenating the plant biodiesels in this study. Furthermore, due to the small scale of reactions performed, accurate isolated yields were not determined for all reactions explored herein. Determination of the purity of the products was beyond the scope of the current



Scheme 2 Schematic illustrations of monomeric pyrazolyl nickel(II) and palladium(II) complexes.⁴²

study, as the sustainable fuel properties were the main focus of this work.

So, complexes **1–6** were evaluated as catalysts for the hydrogenation of methyl linoleate using molecular hydrogen at 0.5 h at 50 °C and 5 bar. Catalytic activities (in terms of the conversion of methyl linoleate) were established in the orders **1** > **3** > **2** for the nickel(II) complexes and **5** > **4** > **6** for the palladium(II) complexes (Table 1). At this temperature and pressure,

five of the six complexes partially hydrogenated the model biodiesel, methyl linoleate (ML), to a mixture of unhydrogenated ML, partially hydrogenated ML and fully hydrogenated ML, except complex **5** which completely hydrogenated ML to methyl stearate (MS), as 'chunky' white solids, in 30 min (Table 1, entry 4; Fig. 1A and S8†).

All six metal complexes were active as catalysts for the hydrogenation of ML as described in (Scheme 3, Table 1, and

Table 1 Catalytic activities of complexes **1–6** for the hydrogenation reaction of methyl linoleate using molecular hydrogen^a

Entry	Complex	Time (h)	Conversion (%)	TON	TOF	Amount of MO detected ^b (%)	Amount of MS detected ^b (%)
1	4	0.5	29	35	70	71	3
2	4	1	52	62	62	48	30
3	4	2	100	120	60	Fully hydrogenated	
4	5	0.5	100	120	240	Fully hydrogenated	
5	6	0.5	20	24	48	80	9
6	6	1	35	42	42	65	21
7	6	2	70	84	44	30	38
8	1	0.5	35	42	84	65	4
9	1	1	38	46	46	62	5
10	1	2	41	49	25	59	6
11	2	0.5	28	34	64	71	2
12	2	1	34	41	41	66	17
13	2	2	46	55	28	54	16
14	3	0.5	29	35	70	71	3
15	3	1	40	48	48	61	8
16	3	2	75	90	45	25	44

^a Reaction conditions: 0.3 mmol of methyl linoleate; 2.5 µmol (0.83 mol%) of complex; 5 mL of methanol; 50 °C; 5 bar. ^b Conversions were estimated by ¹H NMR spectroscopy, using dioxane as an internal standard. Each run was performed in duplicates. TOF in mol_{substrate} mol_{catalyst}⁻¹ h⁻¹



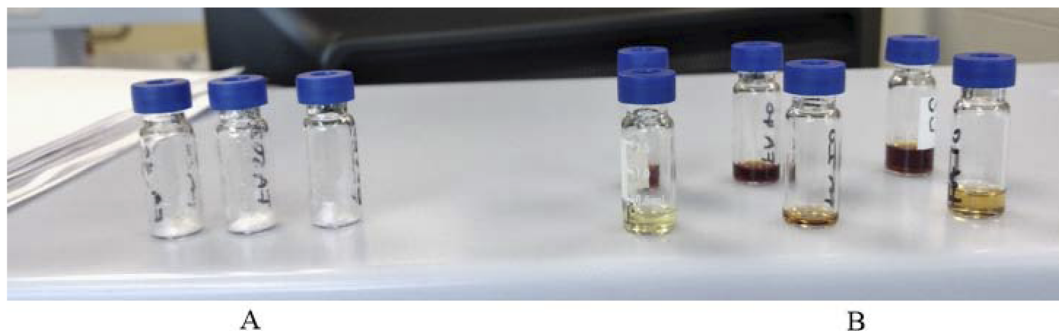
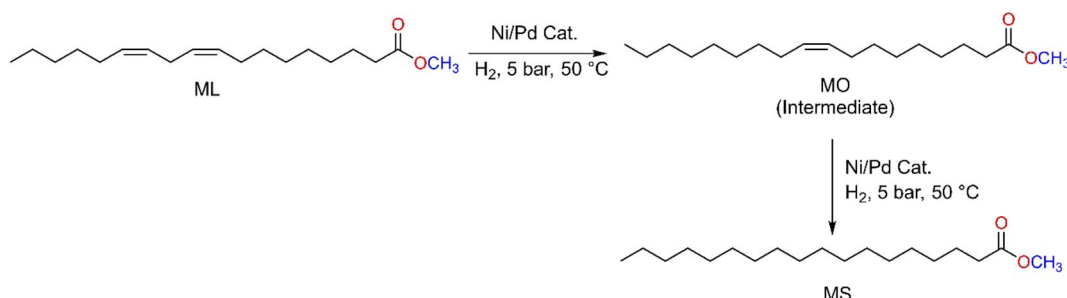


Fig. 1 Hydrogenation of methyl linoleate catalysed by pyrazolyl palladium(II) and nickel(II) complexes using molecular hydrogen. (A) When C=C in methyl linoleate is fully hydrogenated. 39.1 mg of solid was obtained upon hydrogenation of 88.9 mg of oil. (B) When C=C in the methyl linoleyl ester is partially hydrogenated.



Scheme 3 Hydrogenation of methyl linoleate catalysed by pyrazolyl nickel(II) and palladium(II) complexes; showing partially hydrogenated and fully hydrogenated products.

Fig. 2). Of the three palladium complexes (**4–6**), complex **5** completely hydrogenated ML to MS within 0.5 h (Table 1, entry 4 and Fig. S8†), whilst complexes **4** (71%) and **6** (80%) selectively produced methyl oleate (MO) in comparable conversions of 29% and 20% respectively (Table 1, entries 1 and 5; Fig. S3†).

While the selectivity towards MO dropped from 71% at a reaction time of 0.5 h to 48% at 1 h for complex **4** (Table 1, entries 1 and 2), at reaction time 2 h the fully hydrogenated product MS was formed by this complex. Selectivity for complex **6** dropped from 80% at 0.5 h to 65% at 1 h and 30% at 2 h (Table 1, entries

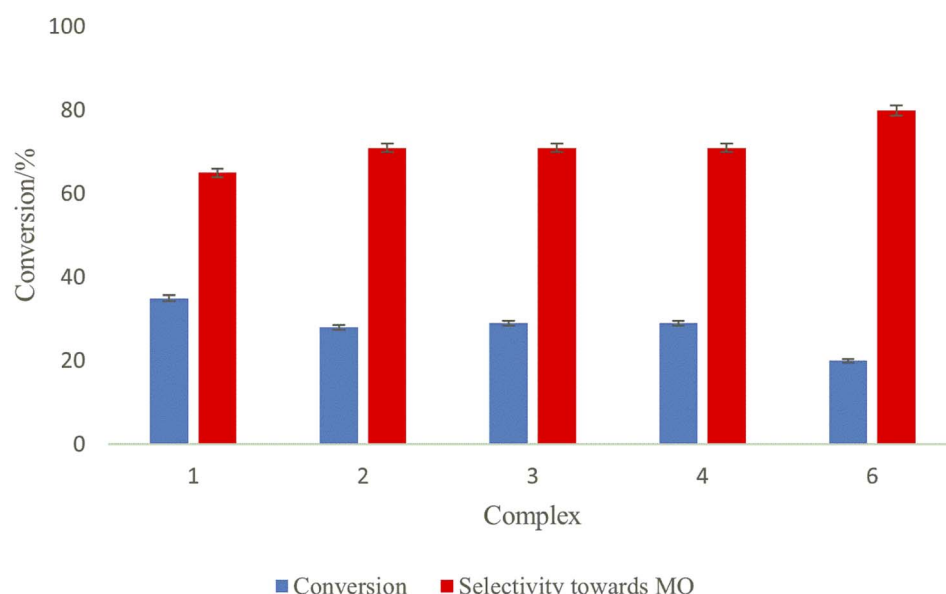


Fig. 2 Hydrogenation of methyl linoleate using molecular hydrogen. ML, 0.3 mmol; complex, 2.5 µmol (0.83 mol%); methanol, 5 mL; 50 °C; 5 bar; 0.5 h. Conversions were estimated by ¹H NMR spectroscopy.

6 and 7) (Fig. S4, S5, and S11†). It is noteworthy that the two C=C bonds in the ML were fully hydrogenated to selectively produce MS after 3 h (Fig. S12†). The nickel complexes (**1–3**), on the other hand, had products that were not fully hydrogenated even after 2 h. For example, complex **1** had only a slight drop in conversion from 65% to 62% from 0.5 h to 1 h reaction time (Table 1, entries 8 and 9) (Fig. S6 and S7†). It is not clear why complex **5** is highly active, although we suspect it could be due to the high solubility of this compound since it has a tertiary-butyl substituent on the pyrazolyl ligand. However, the nickel analogue (complex **2**), has only 28% conversion of ML to MO (71% selectivity) and MS (2% selectivity) when the reaction is run for 0.5 h (Table 1, entry 11). There is an increase in the conversion of ML from 34% (Fig. S9†) up to 46% (Fig. S10†) when the reaction is run from 1 h to 2 h at 5 bar (Table 1, entries 12 and 13). Similar trends were observed with complex **3** as a catalyst, interestingly with higher % conversions of methyl linoleate and much lower selectivity towards MO at 2 h (Table 1, entries 15, 16; Fig. S14 and S15†). It must be noted that Liu *et al.* have reported Pd(0)-PEG nanoparticles that partially hydrogenate methyl linoleate selectively to MO.⁴⁴ The mass spectra for

the ML, partially hydrogenation product (MO) and fully hydrogenated product (MS) are shown in Fig. S16–S18† respectively.

To determine the optimal conditions for the hydrogenation of ML, we investigated the effect of temperature and pressure on the hydrogenation of ML with complex **6** from 40–70 °C and from 5–15 bar and reaction time kept at 1 h (Table S1†). With temperature variation, conversion peaked at 41% when temperature was 60 °C (Table S1,† entries 1–4); however, selectivity for MO dropped from 65% at 50 °C to 59% at 60 °C, and at 70 °C, there was no significant change in the conversion (with 36%) of methyl linoleate and the selectivity (with 64%) towards MO (Table S1, entry 4; Fig. S19†). With pressure variation, conversion continued to increase until it was 100% at 15 bar (Table S1,† entries 2, 5 and 6), but at the expense of MO selectivity which dropped from 65% at 5 bar to 49% at 10 bar and 0% at 15 bar. Therefore, to obtain a mixture of ML, MO and MS, hydrogenation had to be run at 50 °C, and 5 bar to maximise the amount of MO produced. Indeed time-dependent NMR experiments (Fig. 3–5, and S12†) using complex **6** as catalyst provided further support for when the maximum amount of MO was formed during the hydrogenation of ML. The representative of the gas chromatogram showing the

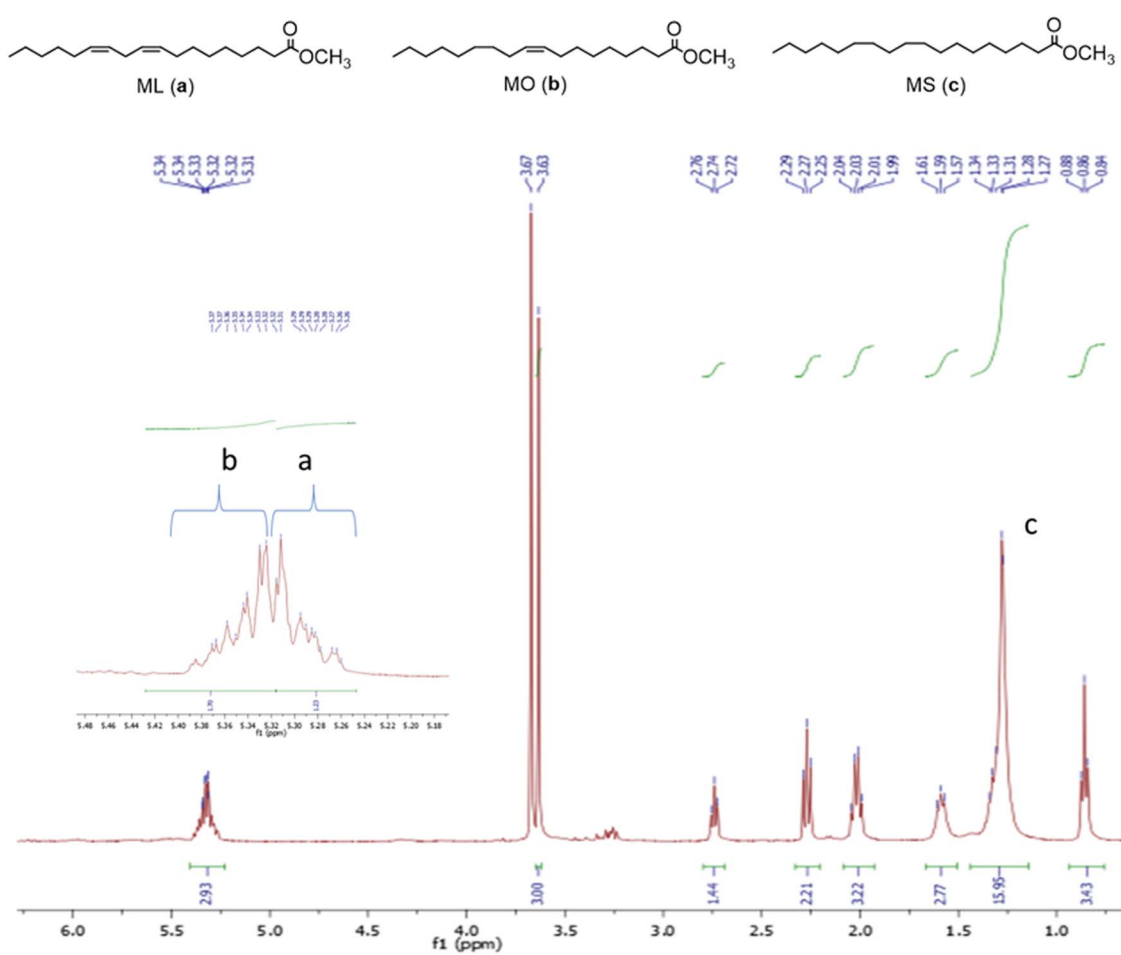


Fig. 3 ^1H NMR spectra of hydrogenation of methyl linoleate (ML) using complex **6** showing the distribution of the product of the MO and MS. 2.5 μmol (0.83 mol%) of the catalyst; 0.3 mmol of methyl linoleate; 5 mL of methanol; 50 °C; 5 bar, 0.5 h. 20% conversion; 80% selectivity towards MO and 9% selectivity towards MS.



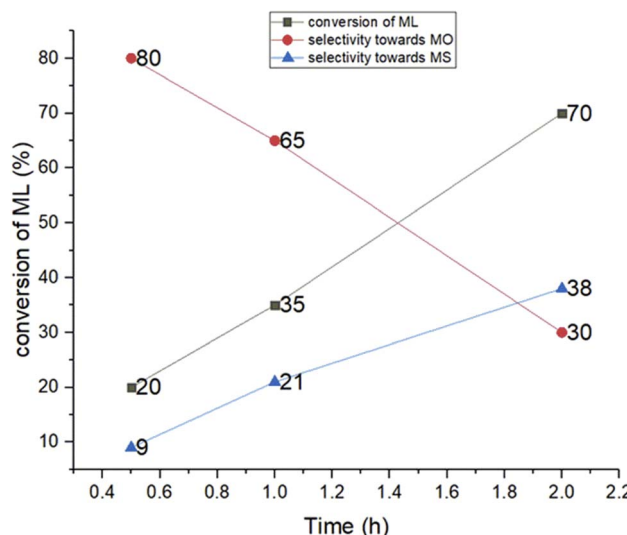


Fig. 4 Time-dependent studies of hydrogenation of ML using 6 as a catalyst. ML, 0.3 mmol; complex 6, 2.5 μ mol (0.8 mol%); methanol, 5 mL; 50 °C; 5 bar. Conversions were estimated by 1 H NMR spectroscopy.

distribution of the products of MO and MS for the hydrogenation of methyl linoleate is shown in Fig. S13.[†]

We were able to establish that the hydrogenation of ML was catalysed homogenously by performing the mercury drop

experiment using complex 6.⁴⁵ Table S1[†] (entries 2 and 7) and Fig. S20[†] provide evidence for this conclusion and that if there were Pd(0) nanoparticles formed during the hydrogenation the amount was minimal.

3.2 Hydrogenation of biodiesel

We were able to use the hydrogenation of ML to determine which catalysts and reaction conditions to use for the hydrogenation of plant biodiesel we prepared. Since complex 5 gave the highest catalytic activity with regards to the hydrogenation of methyl linoleate (Table 1, entry 4), complex 5 and its nickel analogue (complex 2) were evaluated for the partial and/or selective hydrogenation of jatropha, chinaberry and *tsamma* melon seed oil methyl esters. The hydrogenation reactions with complexes 2 and 5 were first screened for 0.5 h at 50 °C and 10 bar. Scheme 4 illustrates the number of C=C bonds in biodiesel. This C=C double bond nomenclature is further used in Tables 2–5 to indicate intermediate compounds that are partially or fully hydrogenated in each plant biodiesel. Methyl ester compositions of biodiesel produced from the three seed oil are shown in (Fig. S23–S25[†]).

It is also important to note that partial and/or selective hydrogenation of polyunsaturated FAME improves the oxidative stability of hydrogenated biodiesel that meets desired fuel properties.⁴⁶ This hydrogenation should lead to minimal C18:3 FAME content in biodiesel since a high amount of C18:3 FAME

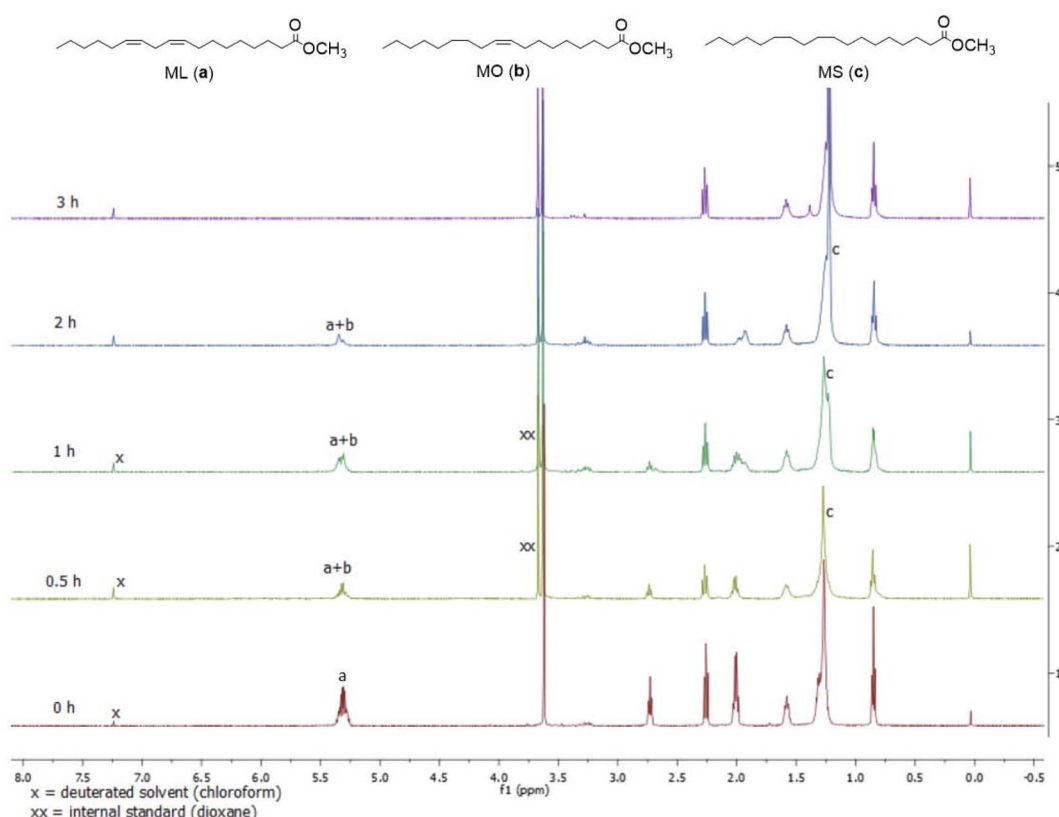
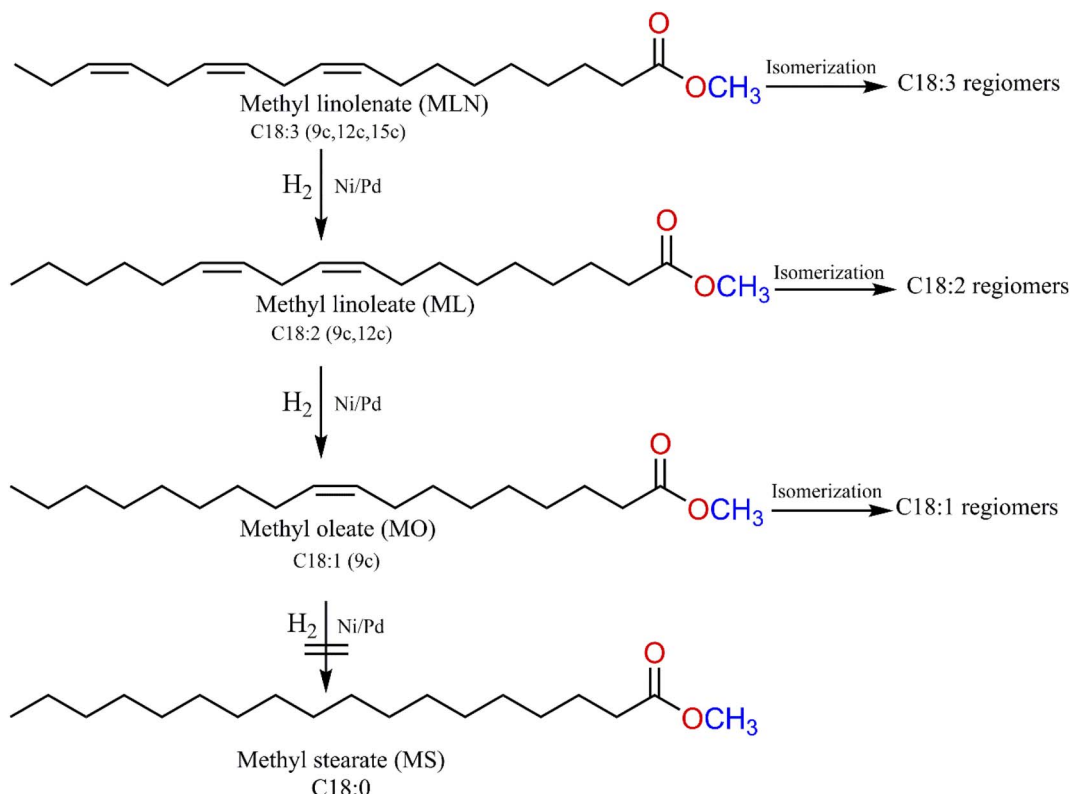


Fig. 5 1 H NMR spectra of hydrogenation of methyl linoleate using complex 6 showing the distribution of the products at different time intervals. 2.5 μ mol (0.83 mol%) of the catalyst; 0.3 mmol of methyl linoleate; 5 mL of methanol; 50 °C; 5 bar.





Scheme 4 Partial/selective hydrogenation of free-fatty acid methyl esters with pyrazolyl nickel(II) and palladium(II) complexes.

Table 2 Methyl ester composition of biodiesel produced from jatropha, chinaberry and *tsamma* melon seed oils^a

FAME/FFA	Jatropha (%)	Chinaberry (%)	<i>Tsamma</i> melon (%)
(9c,12c,15c)-C18:3	5.3	7.8	4.3
(9c,12c)-C18:2	31.4	76.9	47.7
(9c)-C18:1	36.7	0.2	22.6
C18:0	5.8	3.0	11.2
C16:0	14.1	9.3	13
Stearic acid	1.1	n.d	n.d
Palmitic acid	0.5	n.d	n.d
Oleic acid	3.7	n.d	n.d

^a n.d – not detected.

is not suitable for biodiesel formulations. Hence, desirable plant biodiesel products would be products with minimal C18:3 FAME content. This is because the presence of free fatty acid methyl esters containing three or more C=C double bonds impacts oxidative stability since the bis-allylic position is always prone to oxidative attack.⁴⁷

Generally, the hydrogenation of the three plant biodiesels resulted in products with low C18:3 content, while maintaining or improving C18:2 and C18:1 content (Tables 3–5). For example, the hydrogenation of biodiesel produced from jatropha seed oil (JCO) with complex 2 produced MLN (1.5%), ML (23.3%), MO (37.4%), MS (5.6%), with no selectivity towards C18:2 (9c,11t) when the reaction was monitored for 1 h at 50 °C

and 10 bar (Table 3, entry 2) (JCO). It is important to note that the hydrogenation of jatropha methyl esters with complex 2 produced no significant changes in the distribution of the products of polyunsaturated FAME when the reaction was run from 1 h to 3 h at 50 °C and 10 bar (Table 3) (Fig. S26–S28†). These experimental conditions are crucial as they determine when the polyunsaturated FAME preserve a C=C double bond per molecule for biodiesel formulation. After 4 h, the jatropha methyl ester FAME was fully saturated (Table 3, entry 5; Fig. S29†). All the polyunsaturated FAME were converted to monosaturated FAME when the hydrogenation reaction was monitored with complex 5 for 0.5 h at 50 °C and 10 bar, producing mainly 73.4% MS and 1% MO with no selectivity towards C18:2 (9c,11t) (Fig. S30†). In contrast, hydrogenation of the jatropha methyl ester FAME at 25 °C and 10 bar with complex 5 after 0.5 h produced a mixture of MLN (0.5%), ML (26.3%), MO (41.0%) and MS (10.3%) (Fig. S31†); whilst at the same temperature and pressure the hydrogenation products after 1 h gave a mixture of MLN (0.2%), ML (2.3%), MO (58.8%) and MS (16.3%) (Table 3, entries 7 and 8). The effect of the reaction temperature on the partial hydrogenation of biodiesel which affords a significant change in the composition of MLN, ML, and MO offers similar observations as reported by Thunyaratchanon *et al.*⁴⁸ for the partial hydrogenation of soybean oil-derived biodiesel using palladium silica as a catalyst.

Similar trends were observed for the catalytic hydrogenation of both chinaberry and *tsamma* melon seed oil methyl esters (CBO) as compared to the hydrogenation of jatropha methyl

Table 3 Hydrogenation of *Jatropha curcas* methyl esters-JCO^a

Entry	Complex	<i>t</i> (h)	C18:3 (%)	C18:2 (total) (%)	C18:2 (9c,12c) (%)	C18:2 (9c,11t) (%)	C18:1 (%)	C18:0 (%)	TOF ^c (h ⁻¹)
1	Starting feed		5.3	31.4	31.4	—	36.7	5.8	—
2	2	1	1.5	23.3	23.3	—	37.4	5.6	123
3	2	2	1.0	21.3	21.3	—	33.6	5.4	55
4	2	3	0.5	20.1	20.1	—	30.3	6.9	34
5	2	4	—	—	—	—	0.1	75.2	0.2
6	5	0.5	—	—	—	—	1.0	73.4	4
7	5 ^b	0.5	0.5	26.3	26.2	0.1	41.0	10.3	268
8	5 ^b	1	0.2	2.3	2.2	0.1	58.8	16.1	120

^a Reaction conditions: 8.6 µmol of the complex (1 wt%); 0.5 g of JCO; 10 mL of methanol; 50 °C; 10 bar. ^b At 25 °C; 10 bar. Conversions were estimated by gas chromatography. The composition of the FAME was estimated with ~90% match factor. ^c Defined as moles of hydrogenated polyunsaturated FAME units in the C18:3, C18:2 and C18:1 compounds in both the starting feed and other regiomers formed during the reaction per mole of the catalyst (complex) per h.

Table 4 Hydrogenation of chinaberry (*Melia azedarach*) methyl esters-CBO^a

Entry	Complex	<i>t</i> (h)	C18:3 (%)	C18:2 (total) (%)	C18:2 (9c,12c) (%)	C18:2 (9c,11t) (%)	C18:1	C18:0	TOF ^c (h ⁻¹)
1	Starting feed		7.8	76.9	76.9	—	0.2	3.02	—
2	2	0.5	4.4	41.1	41.0	0.1	40.4	4.9	339
3	2	1	0.5	34.3	33.9	0.4	33.5	4.0	135
4	2	2	0.1	20.7	20.5	0.2	54.5	5.2	74
5	5	0.5	—	—	—	—	5.8	66.5	22.78
6	5 ^b	0.5	0.8	31.1	30.9	0.2	23.5	14.5	219
7	5 ^b	1	0.6	2.7	2.7	0.1	50.8	14.7	106

^a Reaction conditions: 8.6 µmol of the complex (1 wt%); 0.5 g of CBO; 10 mL of methanol; 50 °C; 10 bar. ^b At 25 °C; 10 bar. Conversions were estimated by gas chromatography. The composition of the FAME was estimated with ~90% match factor. ^c Defined as moles of hydrogenated polyunsaturated FAME units in the C18:3, C18:2 and C18:1 compounds in both the starting feed and other regiomers formed during the reaction per mole of the catalyst (complex) per h.

esters (JCO) with complexes 2 and 5 (Tables 4 and 5) (Fig. S32–S36†). For the chinaberry methyl ester FAME partial hydrogenation with complex 2 at 50 °C and 10 bar for 0.5 h gave a product mixture of MLN (4.4%), ML (41.0%), MO (40.4%) and MS (4.9%) (CBO) (Fig. S32†); while the most desired partial hydrogenation products mix with the same catalysts and reaction condition for the *tsamma* melon methyl ester was MLN (2.7%), ML (36.6%), MO (40.3%) and MS (14.0%) (MSO)

(Fig. S33†). At a lower temperature, the product distributions of the polyunsaturated FAME were greatly improved using complex 5 when the reaction temperature was reduced to 25 °C at 10 bar, producing 0.8% MLN 30.9% ML, 23.5% MO for the chinaberry methyl ester hydrogenation (Table 4, entry 6) (Fig. S35†) and 0.9% MLN; 36.4% ML, and 20.2% MO for the hydrogenation of *tsamma* melon methyl ester (Table 5, entry 6) (Fig. S36†). Fig. S37† shows a representative gas chromatogram

Table 5 Hydrogenation of *tsamma* melon (*Citrullus ecirrhosus*) methyl esters-MSO^a

Entry	Complex	<i>t</i> (h)	C18:3 (%)	C18:2 (total) (%)	C18:2 (9c,12c) (%)	C18:2 (9c,11t) (%)	C18:1	C18:0	TOF ^c (h ⁻¹)
1	Starting feed		4.3	47.7	47.7	—	22.6	11.2	—
2	2	0.5	2.7	36.6	36.1	0.5	40.3	14.0	314
3	2	1	1.9	38.1	38.0	0.1	31.0	14.2	140
4	2	2	0.1	31.0	30.5	0.5	40.5	14.1	71
5	2	3	—	25.7	15.6	0.1	52.1	14.7	17
6	5 ^b	0.5	0.9	36.7	36.4	0.3	20.2	16.6	228
7	5 ^b	1	0.6	3.5	3.4	0.1	56.9	15.5	120

^a Reaction conditions: 8.6 µmol of the complex (1 wt%); 0.5 g of MSO; 10 mL of methanol; 50 °C; 10 bar. ^b At 25 °C; 10 bar. Conversions were estimated by Gas chromatography. The composition of the FAME was estimated with ~90% match factor. ^c Defined as moles of hydrogenated polyunsaturated FAME units in the C18:3, C18:2 and C18:1 compounds in both the starting feed and other regiomers formed during the reaction per mole of the catalyst (complex) per h.



Table 6 Fuel Properties of the feed biodiesels, partially hydrogenated biodiesels produced with complex 2, at 50 °C, 10 bar and 0.5 h, and conventional diesel fuel^a

Biodiesel/diesel fuel	Cloud point (°C)	Pour point (°C)	Flash point (°C)	Calorific value (MJ kg ⁻¹)	Acid value (mg KOH g ⁻¹)	Density (at 20°C) (kg m ⁻³)
JCO	3.0	2.0	133	42.2	1.58	870
CBO	4.0	2.0	145	44.5	3.22	875
MSO	4.0	2.0	130	41.7	1.22	880
JBH	4.0	3.0	135	39.6	0.23	867
BCB	4.0	2.0	147	43.6	0.35	870
MSB	4.0	3.0	126	42.9	0.10	866
CDF	3.0	-6.0	91	45.6	0.28	845

^a CDF – Conventional diesel fuel.

for the partial hydrogenation of biodiesels from the three seed oils.

3.3 Properties of the biodiesels

We selected partially hydrogenated biodiesels produced with complex 2 catalysed reactions at 50 °C, 10 bar and 0.5 h, as comparable mixtures, to determine the fuel properties to compare them to the un-hydrogenated ones. The properties of the feed biodiesel (JCO, CBO and MSO) and the partially hydrogenated biodiesels (JBH, BCB and MSB); namely, relative density, cold flow properties (cloud and pour points), flash point, calorific value and acid value are presented in Table 6.

These properties were evaluated due to their correlation to improved biodiesel quality and biodiesel formulation *via* partial hydrogenation. The relative density is an important fuel property that directly affects the fuel performance, as some of the engine properties, such as heating value and viscosity, correlate with it. The densities of the partially hydrogenated biodiesel are in the range of 866–870 kg m⁻³ (Table 6), which meet the standard requirement by the European standard EN 14214 for biodiesel as heating oil.

The most significant difference in the properties of our biodiesels compared to the conventional diesel in our study is the cloud point (CP) and pour point (PP). The cloud point (CP) is the temperature at which a fuel becomes cloudy, forming a jelly-like crystal. It is a fuel property that describes the low-temperature operational characteristic of the fuel. At the same time, the pour point (PP) is the temperature at which the fuel contains so many agglomerated crystals that it is essentially a gel and will no longer flow. The cloud points (with an average of 4.0 °C) of the partially hydrogenated FAMEs (*i.e.*, JBH, BCB and MSB) were higher than that for the conventional diesel fuel. These values are lower as compared to the cloud points (with an average of 9.5 °C) reported by Thunyaratchatanon *et al.* for the hydrogenation of soybean oil-based biodiesel using palladium-silica as catalysts.⁴⁸ Similarly, all the partially hydrogenated FAMEs have pour points (with an average of 2.7 °C) higher than that of the conventional diesel fuel. However, no information on the pour points was reported by Thunyaratchatanon *et al.* for the hydrogenation of biodiesel produced from soybean oil.⁴⁸ Although, in another work reported by the same authors for the hydrogenation of biodiesel produced from soybean oil, the

cloud points (with an average of 4.7 °C) are slightly higher with a difference of 0.7 °C. However, the pour points (with an average of -1.2 °C) are lower as compared to our work.⁴⁹ The high CP and PP values of the partially hydrogenated FAME may be due to the high content of the saturated FAME since higher contents of saturated FAME account for higher pour and cloud points.^{38,50} The use of these biodiesels in warm climate countries might not affect the engine, however, for the use of these biodiesels in cold climate countries, the CP and PP might need to be improved by blending with other diesel fuels or adding appropriate chemical additives known as depressants.^{51,52} It is noteworthy that the CP and PP of biodiesels depend on the feedstocks from which the biodiesel is produced.^{38,50}

Flash point (FP) is another critical property that must be considered in assessing the overall flammability hazard of a fuel. It is used to classify fuels for transport, storage, and distribution according to the hazard level.⁵³ The flash points of the partially hydrogenated FAMEs (with an average of 136 °C) are higher than the EN 14214 and ASTM D 6751/D 93 limits of 120 °C and 130 °C, respectively, for conventional diesel fuel. This implies that there is a lower fire hazard that is associated with the use of partially hydrogenated biodiesel as compared to conventional diesel fuel. These results are similar to those reported earlier for peanut oil biodiesel⁵⁴ and jatropha seed oil biodiesel.⁵⁵ The flash points for the un-hydrogenated and the partially hydrogenated biodiesels in our study are higher than the conventional diesel in this study, which is an advantage since these types of diesels are less likely to ignite at normal temperatures found in hot climates compared to conventional diesels.

The heat of combustions or calorific values of the partially hydrogenated FAME, having an average of 42.0 MJ kg⁻¹, is higher than the EN 14214 minimum standard of 35 MJ kg⁻¹ requirement for biodiesel, although lower than the conventional diesel fuel of 45.6 MJ kg⁻¹ (Table 6). The lower calorific values could result from high oxygen content, as reported by Yamane *et al.* that oxygen in fuel improves the combustion properties and emissions but reduces the calorific value.⁵⁶

Another significant property improvement for the partially hydrogenated biodiesel is its acid values, comparable to conventional diesel. Acid value describes the free fatty acids (FFAs) in the biodiesels. Higher acid values in biodiesel cause



operational problems, such as corrosion and fuel clogging by deposit formation.³⁸ The acid values (0.10–0.35 mg KOH/g) presented in Table 6 for the three partially unsaturated FAMEs are within the specifications of EN 14214 and ASTM D6751.

4 Conclusion

We have used pyrazolyl nickel(II) and palladium(II) complexes to establish their ability to selectively hydrogenate methyl linoleate and biodiesel produced from jatropha, chinaberry and melon seed oils. Catalytic activities (in terms of the conversion of methyl linoleate) are in the orders of **1** > **3** > **2** and **5** > **4** > **6** for the nickel(II) and palladium(II) complexes, respectively. The hydrogenation is generally homogeneous as demonstrated with complex **6** and selective towards the C=C bonds over the carbonyl (C=O) moiety.

It is significant to note that the bulk properties of the mixture of un-hydrogenated, partially hydrogenated, and fully hydrogenated of the three plant biodiesels in this study meet major international standards such as EN 14214 and ASTM D 6751. These include lower fire hazard compared to conventional diesel fuel and highly improved acid values compared to their un-hydrogenated biodiesels. Lastly, our study shows that if the desired product from the hydrogenation of the FAMEs studied in this report is to produce wax, then complex **5** can be used to make such waxes.

Author contributions

Oluwasegun E. Olaoye: investigation; formal analysis; methodology. Olayinka Oyetunji: conceptualization; funding acquisition; supervision; formal analysis; resources. Banothile C. E. Makhubela: conceptualization; supervision; formal analysis; resources. Gopendra Kumar: supervision; funding acquisition. James Darkwa: conceptualization; supervision; formal analysis; resources.

Conflicts of interest

The authors declare no conflict of interest.

Acknowledgements

The authors are grateful for the funding provided by the Royal Society-Foreign Commonwealth and Development Office (RSFCDO), United Kingdom. (Registered Charity Number 207043).

References

- 1 S. Alexander, V. Udayakumar and V. Gayathri, *J. Mol. Catal.*, 2009, **314**, 21–27.
- 2 Y. Liu, I. D. Gridnev and W. Zhang, *Angew. Chem., Int. Ed.*, 2014, **53**, 1901–1905.
- 3 G. Amenuvor, B. C. E. Makhubela and J. Darkwa, *ACS Sustain. Chem. Eng.*, 2016, **4**, 6010–6018.
- 4 R. A. Farrar-tobar, Z. Wei, H. Jiao, S. Hinze and J. G. De Vries, *Chem.-Eur. J.*, 2018, **24**, 2725–2734.
- 5 T. A. Tshabalala and S. O. Ojwach, *J. Organomet. Chem.*, 2018, **873**, 35–42.
- 6 S. Naskar and M. Bhattacharjee, *Tetrahedron Lett.*, 2007, **48**, 465–467.
- 7 S. Bauri, S. N. R. Donthireddy, P. M. Illam and A. Rit, *Inorg. Chem.*, 2018, **57**, 14582–14593.
- 8 D. Spasyuk, S. Smith and D. G. Gusev, *Angew. Chem., Int. Ed.*, 2012, **51**, 2772–2775.
- 9 G. Zhang, Z. Yin and J. Tan, *RSC Adv.*, 2016, **6**, 22419–22423.
- 10 P. Wang, H. Liu, M. Liu, R. Li and J. Ma, *New J. Chem.*, 2014, **38**, 1138–1143.
- 11 G. Shang, W. Li and Z. Zhang, in *Catalytic Asymmetric Synthesis*, John Wiley and Sons, New York, 3rd edn, 2010.
- 12 F. Nerozzi, *Plat. Met. Rev.*, 2012, **56**, 236–261.
- 13 E. Bouwman, *Handbook of Homogeneous Hydrogenation*, Wiley-VCH Verlag GmbH and Co. KGaA, Weinheim, 2007.
- 14 Z. R. Dong, Y. Y. Li, S. L. Yu, G. S. Sun and J. X. Gao, *Chin. Chem. Lett.*, 2012, **23**, 533–536.
- 15 Y. Y. Li, S. L. Yu, W. Y. Shen and J. X. Gao, *Acc. Chem. Res.*, 2015, **48**, 2587–2598.
- 16 R. J. Liua, P. A. Croziera, C. M. Smith, D. A. Hucule, J. Blackson and G. Salaita, *Appl. Catal. Gen.*, 2005, **282**, 111–121.
- 17 I. M. Angulo, A. M. Kluwer and E. Bouwman, *Chem. Commun.*, 1998, 2689–2690.
- 18 I. M. Angulo and E. Bouwman, *J. Mol. Catal. A: Chem.*, 2001, **175**, 65–72.
- 19 I. M. Angulo, E. Bouwman, R. van Gorkum, S. M. Lok, M. Lutz and A. L. Spek, *J. Mol. Catal. A: Chem.*, 2003, **202**, 97–106.
- 20 M. Shevlin, M. R. Friedfeld, H. Sheng, N. A. Pierson, J. M. Hoyl, L. C. Campeau and P. J. Chirik, *J. Am. Chem. Soc.*, 2016, **138**, 3562–3569.
- 21 E. Negishi, *Handbook of Organopalladium Chemistry for Organic Synthesis*, Wiley and Sons, New York, 2002.
- 22 F. A. Harraz, S. E. El-Hout, H. M. Killa and I. A. Ibrahim, *J. Catal.*, 2012, **286**, 184–192.
- 23 P. Pelagatti, A. Bacchi, M. Carcelli, M. Costa, A. Fochi, P. Ghidini, E. Leporati, M. Masi, C. Pelizzi and G. Pelizzi, *J. Organomet. Chem.*, 1999, **583**, 94–105.
- 24 A. Bacchi, M. Carcelli, M. Costa, A. Leporati, E. Leporati, P. Pelagatti, C. Pelizzi and G. J. Pelizzi, *Organomet. Chem.*, 1997, **535**, 107–120.
- 25 B. Ding, Z. Zhang, Y. Liu, M. Sugiya, T. Imamoto and W. Zhang, *Org. Lett.*, 2013, **15**, 3690–3693.
- 26 M. Boronat, A. Corma, C. González-Arellano, M. Iglesias and F. Sánchez, *Organometallics*, 2010, **29**, 134–141.
- 27 M. W. Van Laren and C. J. Elsevier, *Angew. Chem., Int. Ed.*, 1999, **38**, 3715–3717.
- 28 S. H. Teo, A. Islam and Y. H. Taufiq-Yap, *Chem. Eng. Res. Des.*, 2016, **111**, 362–370.
- 29 B. Aghabarari, N. Dorostkar and M. V. Martinez-Huerta, *Fuel Process. Technol.*, 2014, **118**, 296–301.
- 30 Y. A. Elsheikh, *Process Saf. Environ. Prot.*, 2014, **92**, 828–834.
- 31 M. S. M. Zaharin, N. R. Abdullah, G. Najafi, H. Sharudin and T. Yusaf, *Renew. Sustain. Energy Rev.*, 2017, **79**, 475–493.



32 N. Rasimoglu and H. Temur, *Energy*, 2014, **68**, 57–60.

33 J. Elguero and E. J. R. Jacquier, *Bull. Soc. Chim. Fr.*, 1968, **2**, 707–711.

34 K. Niedenzu, J. Sorwatowski and S. Trofimenko, *Inorg. Chem.*, 1991, **30**, 524–527.

35 G. K. Anderson, M. Lin, A. Sen and E. Gretz, *Inorg. Synth.*, 1990, **28**, 60–63.

36 E. Ocansey, J. Darkwa and B. C. E. Makhubela, *Polyhedron*, 2019, **166**, 52–59.

37 S. M. Nelana, J. Darkwa, I. A. Guzei and S. F. Mapolie, *J. Organomet. Chem.*, 2004, **689**, 1835–1842.

38 G. Knothe, *J. Am. Oil Chem. Soc.*, 2006, **83**, 823–833.

39 K. Li, J. Darkwa, I. A. Guzei and S. F. Mapolie, *J. Organomet. Chem.*, 2002, **660**, 108–115.

40 K. Li, M. S. Mohlala, T. V. Segapelo, P. M. Shumbula, I. A. Guzei and J. Darkwa, *Polyhedron*, 2008, **27**, 1017–1023.

41 F. K. Keter, S. Kanyanda, S. Lyantagaye, J. Darkwa, J. Rees and M. Meyer, *Cancer Chem. Pharm.*, 2008, **63**, 127–138.

42 (a) O. E. Olaoye, O. Oyetunji, B. C. E. Makhubela, A. Muyaneza, G. Kumar and J. Darkwa, *S. Afr. J. Chem.*, 2021, **74**, 50–56; (b) C. C. Chou, C. C. Yang, H. B. Syu and T. S. Kuo, *J. Organomet. Chem.*, 2013, **745–746**, 387–392; (c) E. Ocansey, J. Darkwa and B. C. E. Makhubela, *RSC Adv.*, 2018, **8**, 13826–13834; (d) E. Ocansey, J. Darkwa and B. C. E. Makhubela, *Polyhedron*, 2019, **166**, 52–59; (e) A. Sanchez-Mendez, E. de Jesus, J. C. Flores and P. Gomez-Sal, *Eur. J. Inorg. Chem.*, 2010, 1881–1887.

43 P. Tolvanen, T. Kilpiö, P. Mäki-Arvela, D. Y. Murzin and T. Salmi, *ACS Sustain. Chem. Eng.*, 2014, **2**, 537–545.

44 W. Liu, L. Xu, G. Lu and H. Zhang, *ACS Sustain. Chem. Eng.*, 2017, **5**, 1368–1375.

45 G. M. Whitesides, M. Hackett, R. L. Brainard, J. P. M. Lavalleye, A. F. Sowinski, A. N. Izumi, S. S. Moore, D. W. Brown and E. M. Staudt, *Organometallics*, 1985, **4**, 1819–1830.

46 F. Zaccheria, R. Psaro, N. Ravasio and P. Bondioli, *Eur. J. Lipid Sci. Technol.*, 2012, **114**, 24–30.

47 A. Bouriazo, C. Vasiliou, A. Tsichla and G. Papadogianakis, *Catal. Today*, 2015, **247**, 20–32.

48 C. Thunyarat chatanom, J. Jitjamnong, A. Luengnaruemitchai, N. Numwong, N. Chollacoop and Y. Yoshimura, *Appl. Catal. A*, 2016, **520**, 170–177.

49 C. Thunyarat chatanom, A. Luengnaruemitchai, J. Jitjamnong, N. Numwong, N. Chollacoop, S.-Y. Chen and Y. Yoshimura, *Energy Fuels*, 2018, **32**, 9744–9755.

50 I. Barabás and I. A. Todoruț, *Biodiesel Quality, Standards and Properties, Biodiesel- Quality, Emissions and By-Products*, InTech, Shanghai, 2011.

51 V. Makareviciene, K. Kazancev and I. Kazanceva, *Renew. Energy*, 2015, **75**, 805–807.

52 S. Nainwal, N. Sharma, A. S. Sharma, S. Jain and S. Jain, *Energy*, 2015, **89**, 702–707.

53 A. M. Ashraful, H. H. Masjuki, M. A. Kalam, I. M. Rizwanul Fattah, S. Imtenan, S. A. Shahir and H. M. Mobarak, *Energy Convers. Manag.*, 2014, **80**, 202–228.

54 M. Ahmad, S. Rashid, M. A. Khan, M. Sultan and S. Gulzar, *Afr. J. Biotechnol.*, 2009, **8**, 441–443.

55 P. K. Barua, *Int. J. Energy Inform. Commun.*, 2011, **2**, 63–65.

56 K. Yamane, A. Ueta and Y. Shimamoto, *Int. J. Engine Res.*, 2001, **4**, 249–261.

